Direct Observation of Molecular Orbitals in an Individual Single-Molecule Magnet Mn_{12} on Bi(111)

Kai Sun,[†] Kyungwha Park,[‡,*] Jiale Xie,[†] Jiyong Luo,[†] Hongkuan Yuan,[†] Zuhong Xiong,[†] Junzhong Wang,[†,*] and Qikun Xue[§]

[†]School of Physical Science and Technology & MOE Key Lab Luminescence & Real Time Analysis, Southwest University, Chongqing 400715, China, [‡]Department of Physics, Virginia Tech, Blacksburg, Virginia 24061, United States, and [§]Department of Physics, Tsinghua University, Beijing 10084, China

ABSTRACT Single-molecule nanomagnets have unique quantum properties, and their potential applications require characterization and accessibility of individual single-molecule magnets on various substrates. We develop a gentle tip-deposition method to bring individual prototype single-molecule magnets, manganese-12-acetate (Mn_{12}) molecules, onto the semimetallic Bi(111) surface without linker molecules, using low-temperature scanning tunneling microscopy. We are able to identify both the almost flat-lying and side-lying orientations of Mn_{12} molecules at 4.5 K. Energy-resolved spectroscopic mapping enables the first observation of several molecular orbitals of individual Mn_{12} molecules in real space, which is consistent with density functional theory calculations. Both experimental and theoretical results suggest that an energy gap between the highest occupied molecular orbital (HOMO) and the lowest unoccupied molecular orbital (LUMO) of the almost flat-lying Mn_{12} is only 40% of such a gap for an isolated (free) Mn_{12} molecule, which is caused by charge transfer from the metallic surface states of Bi to the Mn_{12}. Despite the reduction of this gap, STM images show that the local lattices of Bi(111) covered with Mn_{12} remain essentially intact, indicating that Mn_{12}—Bi interactions are not strong. Our findings open an avenue to address directly the local structural and electronic properties of individual single-molecule magnets on solid substrates.

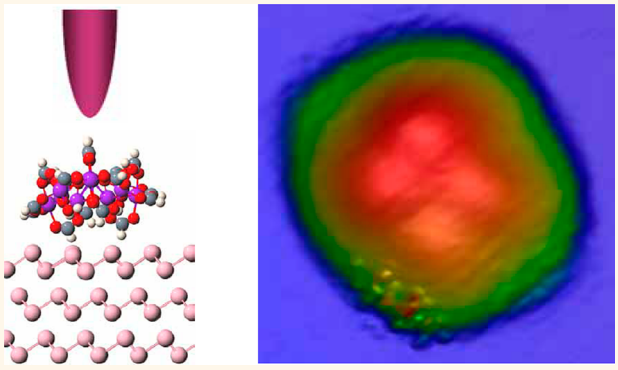

KEYWORDS: STM · single-molecule magnet · semimetal Bi · tip deposition · molecule–substrate interaction · density functional theory

Single-molecule magnets (SMMs) are nanoscale molecules with unique properties such as quantum tunneling of magnetization and quantum phase interference (Berry phase oscillations), which could be used for potential applications for information storage, molecular spintronics, or quantum computation.[1−4] Such device applications demand SMMs adsorbed on solid substrates with their electronic structures and magnetic properties well-characterized, as well as accessibility of individual SMMs. Along this rationale, a great effort has been made to deposit various SMMs, such as Mn_{12},[5−11] Mn_6,[12] Fe_4,[13] and Cr_7Ni,[14,15] on metallic or semiconducting substrates or to form single-molecule junctions or transistors comprising SMMs bridged between electrodes.[16−20]

A prototype SMM Mn_{12}, $[Mn_{12}O_{12}(COOCH_3)_{16}(H_2O)_4]$, consists of a $Mn_{12}O_{12}$ core surrounded by 16 acetate groups (Figure 1a). It exhibits the highest blocking temperature due to the large magnetic anisotropy barrier. The conventional vacuum sublimation method turned out to be inadequate due to thermal instability and fragileness of Mn_{12} molecules. Thus, the solution-based deposition was employed in most experiments. A major drawback of this technique is that Mn_{12} molecules easily aggregate into disordered monolayers, making individual SMMs inaccessible. Recently, there have been successful attempts to deposit individual SMMs on surfaces, such as the eletrospray deposition[7,11] or mechanical dry-imprint method.[21]

In the previous effort to deposit Mn_{12} molecules on surfaces, the following important question was raised: Do the Mn_{12} molecules deposited on solid surfaces remain

* Address correspondence to kyungwha@vt.edu, jzwangcn@swu.edu.cn.

Received for review April 14, 2013 and accepted July 7, 2013.

Published online July 08, 2013
10.1021/nn401827h

intact, or are they broken into smaller clusters? The answer to this question critically relies on activities of solid substrates as well as gentleness of deposition techniques. A majority of experiments utilized either noble metal substrates such Au[8−12] or inert insulating substrates such as SiO_2.[22] In the former case, Mn_{12}−substrate interactions may be strong due to large electron density of states (DOS) at the Fermi level E_F, and so the electronic structure and magnetic properties of Mn_{12} can be greatly modified. In the latter case, the Mn_{12}−substrate interactions are so weak that the deposited Mn_{12} molecules are highly mobile on the substrates, leading to disordered aggregations even at submonolayer coverage. An interesting case is between these two regimes such as semimetallic substrates, where molecule−substrate interactions are, in general, weaker than those for metallic substrates, yet stronger than those for inert insulating substrates. (This implies that some charge transfer may be allowed for semimetallic substrates.) Thus, we expect both moderate molecule−substrate interactions and individual accessibility of Mn_{12} molecules on semimetallic substrates. Recently, thin films of pentacene molecules epitaxially grown on semimetallic Bi(111) have been shown to form an ordered crystalline layer with the standing-up orientation rather than the planar orientation on Au(111).[23] This newly formed orientation arises due to moderate molecule−Bi interactions (because of smaller DOS of Bi near E_F than that of Au)[24,25] competing with pentacene−pentacene interactions.

So far, almost all the experiments have been performed to measure spatially averaged electronic structures of Mn_{12} on surfaces due to molecular aggregations. Neither individual molecular orbitals nor spatial mapping of local DOS has been characterized for isolated Mn_{12} molecules on surfaces. As discussed earlier, it is crucial to have capability of probing electronic structures of individual SMMs. Low-temperature scanning tunneling microscopy and spectroscopy (LT-STM/STS) are powerful techniques to probe and address individual SMMs in real space with a judicious choice of deposition methods.

Here we develop a gentle tip-deposition method to bring individual Mn_{12} molecules onto the semimetal Bi(111) surface at low temperature (78 K). Figure 1b illustrates how individual Mn_{12} molecules are transferred from a Mn_{12} aggregation to a clean Bi(111) surface. Two typical molecular orientations (almost flat-lying and side-lying) have been identified with LT-STM at 4.5 K. Differential conductance (d*I*/d*V*) maps have been first measured for the individual Mn_{12} molecules on Bi(111). Our findings open an avenue to directly characterize the local electronic structures of individual SMMs on semimetallic substrates.

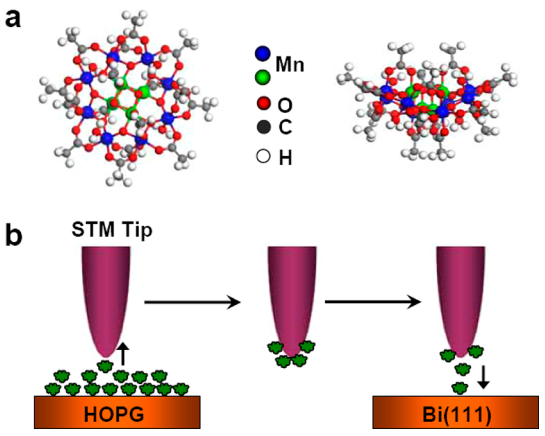

Figure 1. (a) Top-down (left) and side-on (right) views of the chemical structure of a Mn_{12} molecule. (b) Schematic view of the tip-deposition technique.

RESULTS AND DISCUSSION

A representative topographic image for tip-deposited Mn_{12} molecules on Bi(111) is shown in Figure 2a. Individual Mn_{12} molecules are randomly distributed on Bi(111) within an area of several hundred square nanometers. The lateral spacing between the Mn_{12} molecules varies from several to tens of nanometers, depending on tip-pulse times. The apparent molecular height varies from 4.5 to 7.0 Å, very close to the reported heights of Mn_{12} molecules deposited on Au or BN.[7,11] (It was shown that the magnetic cores of Mn_{12} molecules on BN remain intact.[7]) The varying heights of the molecules can be attributed to different orientations of the individual Mn_{12} with respect to the Bi substrate. In addition, there are some smaller clusters with an

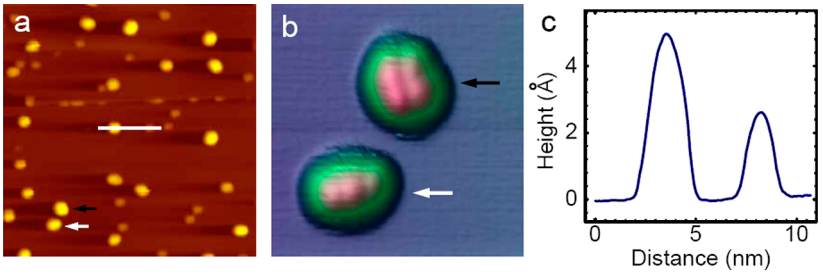

Figure 2. (a) STM image of individual Mn_{12} molecules grafted on the Bi(111) surface by the tip-deposition technique (50 × 50 nm^2, 2.0 V). The black and white arrows mark the two Mn_{12} molecules with almost flat-lying and side-lying orientations, respectively. (b) Close-up view of the two Mn_{12} molecules marked with the arrows in (a) (7.5 × 7.5 nm^2, 0.5 V). (c) Cross-sectional profile line along the solid line shown in (a).

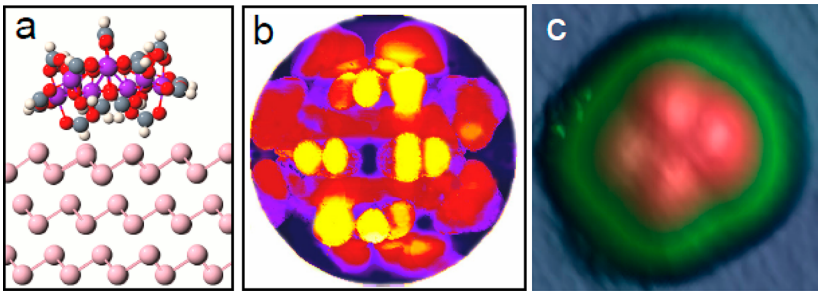

Figure 3. (a) Side view of the optimized flat-lying Mn_{12} on Bi(111). (b) Simulated topographic image of a flat-lying Mn_{12} using the DFT+U method at 1.5 eV. (c) High-resolution STM image of a flat-lying Mn_{12} (36 × 36 Å^2, 1.5 V).

apparent height around 2.7 Å. These clusters are identified as IPA solvent molecules, when they are compared with STM images of pristine IPA solvent adsorbed on Bi(111) using the same tip-deposition method (see Supporting Information, Figure S1).

To examine adsorption geometries of the individual Mn_{12} molecules on Bi, we have analyzed several bright spots corresponding to Mn_{12} molecules in Figure 2a and in another batch of samples, using high-resolution STM at 4.5 K. From the lateral sizes of the Mn_{12} molecules in such a high-resolution STM image (Figure 2b), we have identified two distinct Mn_{12} orientations: one is an almost flat-lying orientation (Figure 3a), which exhibits a circular cross section with a diameter of 2.5 ± 0.2 nm (marked by the black arrow in Figure 2b), corresponding to the roughly planar disk-like Mn_4O_4 cubane (Mn^{4+}) surrounded by eight Mn^{3+} ions; the other is a side-lying orientation (Figure S3b) exhibiting an oval cross section with a long axis of 2.5 ± 0.2 nm and a short axis of 1.8 ± 0.2 nm (marked by the white arrow in Figure 2b). As displayed in Figure 1a, a Mn_{12} molecule has eight CH_3 groups normal to the plane of the disk and the rest of eight CH_3 groups on the equator of the molecule. Since the magnetic easy axis of a Mn_{12} molecule is perpendicular to the disk plane, for the almost flat-lying (side-lying) orientation, the easy axis is very close to normal (parallel) to the substrate surface. The topographic image corresponding to the almost flat-lying orientation in Figure 2b reveals four protrusions on top of the Mn_{12} molecule, where each protrusion corresponds to a CH_3 group. In this case, the four protrusions reveal four-fold symmetry and slightly different brightness, indicating small tilting of the Mn_{12} molecule relative to the surface or from the completely flat-lying orientation. From Figure 2a, we can also infer that the circular cross sections are for almost flat-lying Mn_{12} molecules, and the oval cross sections represent side-lying or rotated Mn_{12} molecules. Figure 2a, however, cannot provide as detailed adsorption structures as Figure 2b. We confirmed that all the examined high-resolution STM images with circular cross sections are similar to the top image in Figure 2b. Besides the two orientation types, there are some tilted or rotated orientations where individual Mn_{12} molecules are deposited onto the substrate with a variety of slant angles or with their magnetic easy axes significantly tilted from normal or parallel to the substrate surface. Statistically, we found that about 10% of the deposited Mn_{12} molecules form dimers. Among the observed individual Mn_{12} molecules, 50 and 20% have almost flat-lying and side-lying orientations, respectively, while the remaining 30% have significantly tilted or rotated orientations. Henceforth, we focus on a Mn_{12} molecule in the almost flat-lying Mn_{12} orientation. (For a short description of observed and calculated results for the side-lying orientation, see Supporting Information.) We observed only elastic tunneling (not spin-flip) processes because the temperature was not low enough. In the almost flat-lying orientation, the tilting of the Mn_{12} molecule relative to the surface is very small (such as about 6° obtained from the cross-sectional profile of the observed STM image), and so hereafter such orientation is simply called the flat-lying orientation.

To understand the coupling nature of the Mn_{12} with a Bi substrate, we have simulated Mn_{12} molecules adsorbed on a Bi(111) slab, using the DFT+U method[26] including spin−orbit coupling (SOC) and dipole corrections. In the optimized flat-lying structure (Figure 3a), the Mn_{12} molecule remains slightly tilted such that its easy axis is tilted by 6° from the normal axis of the Bi(111) surface. To simulate a topographic STM image of the Mn_{12} on Bi, molecular orbitals were integrated from E_F to 1.5 eV above E_F, using the Tersoff−Hamann approach.[27,28] The simulated STM image shows four bright protrusions with almost four-fold symmetry on top of the flat-lying Mn_{12} (Figure 3b), which is consistent with the high-resolution STM image in Figure 3c.

To understand the local electronic structure of the Mn_{12} molecules on Bi, d*I*/d*V* spectra have been measured at five different spots over a single flat-lying Mn_{12} molecule adsorbed on a Bi(111) surface (Figure 4). To ensure measurements with clean STM tips, d*I*/d*V* spectra were first recorded on pristine Bi(111), and only tips yielding spectral signatures corresponding to bare Bi(111) were used. Based on the measurement over ~30 Mn_{12} molecules, six peaks were observed in the range of ±1.0 V, where the amplitudes did not

show strong variation over the Mn_{12} surface. The HOMO−LUMO gap was measured to be 0.40 eV with the HOMO and LUMO levels at −0.37 and 0.03 ± 0.01 eV, respectively. This result is close to our DFT+U calculated values (−0.39 V for the HOMO and 0.04 V for the LUMO,[29] Figure S5a). Our measured HOMO−LUMO gap is only 40% of the experimental gap (~1 eV) for a Mn_{12} crystal[30] or for cases where the Mn_{12}−substrate interactions are negligible.[5−7] The reduction of the gap may be attributed to charge transfer from the Bi(111) to the molecule. Although Bi is a semimetal, significant electron density exists near E_F arising from metallic surface states. The charge transfer causes the LUMO level of a free Mn_{12} to be occupied, and thus it creates a smaller apparent HOMO−LUMO gap for the adsorbed Mn_{12}. Despite the apparent reduction of the HOMO−LUMO gap, the Mn_{12}−Bi interactions are not so strong that the Bi(111) lattice remains essentially intact upon removal of the Mn_{12} molecules (Supporting Information, Figure S2). Thus, strong chemical bonding can be excluded for the Mn_{12} molecules adsorbed on the semimetallic Bi(111) substrate. (Figure S2 also excludes any possibility of asymmetric STM tips.) Moreover, within the HOMO−LUMO gap, we found a smaller peak located at −0.17 V, which can be assigned to the surface states of the Bi(111) film.[31,32] This assignment agrees with our DFT+U calculations (Supporting Information, Figure S5a).

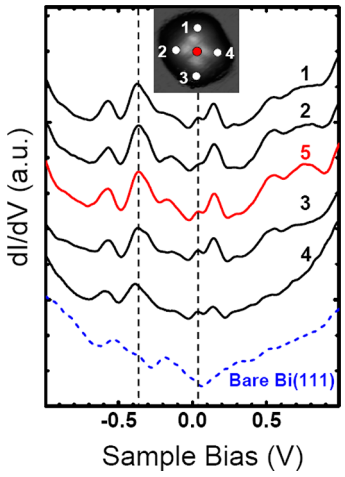

Figure 4. d*I*/d*V* spectra of a flat-lying Mn_{12} molecule. Spectra 1−5 were taken at the indicated spots in the inset image and were vertically shifted for clarity. The vertical tip position corresponds to the feedback parameters of current *I* = 0.1 nA and bias voltage *U* = 2.0 V. The lowest spectrum was obtained on the bare Bi(111) surface. The vertical dashed lines correspond to the HOMO and LUMO levels.

To explore two-dimensional spatial distributions of electron density, we performed energy-resolved spectral mapping of molecular orbitals for the flat-lying Mn_{12} (Figure 3c) at 4.5 K. Figure 5a−e shows the spectral mapping taken at the resonant energies in the STS curve of the flat-lying Mn_{12}, where Figure 5c,d represents the LUMO and HOMO, respectively. Comparing the calculated LDOS in Figure 5f−j, we find that the bright lobe at the center of Figure 5b is attributed to the localized electrons at the inner Mn ions, while the bright lobes in Figure 5a,c−e originate from the outer Mn ions. Overall, the observed spectral mapping agrees with the calculated LDOS at each resonant energy. Our calculation suggests that the small tilting in the almost flat-lying orientation allows some Mn ions to be closer to the surface, inducing asymmetric charge transfer from the Bi substrate to the Mn_{12}. We find that the Mn site with the large electron density as shown in Figure 5d,i is the closest to the Bi surface among the Mn sites contributing to the LUMO of a free Mn_{12}. Thus, the charge transfer occurs mostly from the Bi substrate to this Mn site (indicated as empty square in Figure S6c) upon adsorption. This is consistent with the observation that Figure 5d corresponds to the HOMO. Figure S6 shows projected DOS and orbital analysis, which corroborate the asymmetric charge transfer scenario. The high asymmetry in the observed spectral mapping

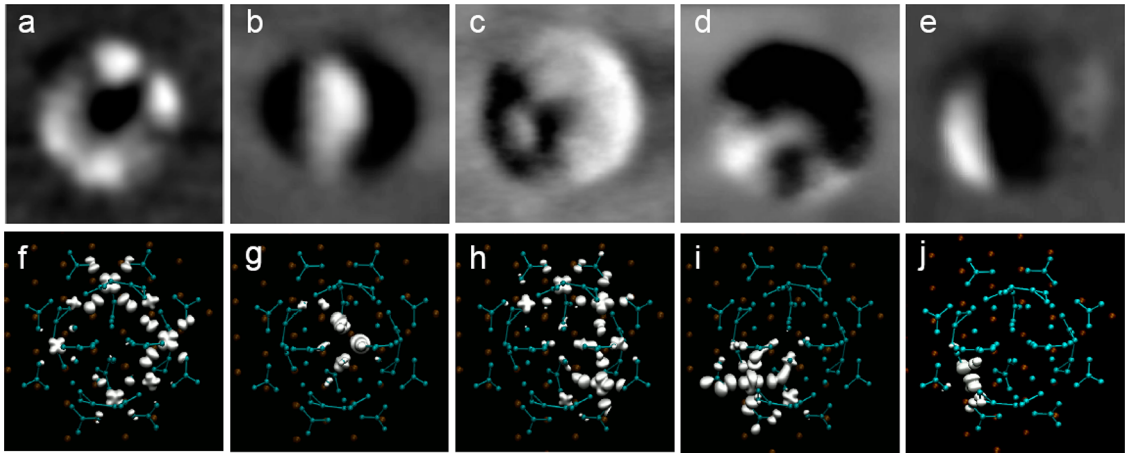

Figure 5. Comparison of experimental STS images of the flat-lying Mn_{12} molecule with theory. (a−e) d*I*/d*V* mapping taken at *U* = 0.53, 0.16, 0.03, −0.37, and −0.57 V, respectively, with *I* = 0.08 nA. (f−j) Simulated LDOS of the flat-lying Mn_{12} at *E* = 0.51, 0.33, 0.04, −0.39, and −0.68 eV, respectively, with an isovalue of 0.01 e/Å^3.

and the calculated LDOS also supports the asymmetric charge transfer.

CONCLUSIONS

In summary, we have anchored individual Mn_{12} molecules on a semimetallic Bi(111) surface *via* a gentle tip-deposition method. Two typical orientations of Mn_{12} molecules have been discerned from high-resolution STM images. Almost flat-lying Mn_{12} molecules reveal a reduced HOMO−LUMO gap of 0.40 eV. Energy-resolved d*I*/d*V* maps were first measured for the individual Mn_{12} molecules adsorbed on Bi(111) with LT-STM/STS. The observed d*I*/d*V* maps agree with the DFT+U calculations. Our results provide direct information on the local structure and electronic properties of individual Mn_{12} on a semimetallic substrate.

METHODS

Experimental Methods. Experiments were conducted in a Unisoku LT-STM 1500 system. A Bi(111) film of 10−12 monolayers was prepared by depositing Bi atoms on a Si(111)-7 × 7 surface with subsequent annealing at 120 °C. The d*I*/d*V* spectra were measured through lock-in detection of the ac tunneling current modulated by a 2505 Hz, 15 mV signal added to the junction bias under open-loop conditions. All the images and spectra data were acquired at either 4.5 or 78 K. Mn_{12} molecules were synthesized as described by Lis.[33] Mn_{12} crystals were dissolved into isopropyl alcohol (IPA) solvent. The Mn_{12} solution was dropped onto the HOPG surface in a load-lock chamber with N_2 gas flowing out. After solvent sublimation by rotary pumping, the sample was transferred into a UHV-STM chamber. A STM tungsten (W) tip was employed to deposit individual Mn_{12} molecules on a Bi(111) surface through a bias pulse of 5 V. Before the tip pulse, the same STM tip was used to scan the Mn_{12} monolayer on HOPG. Many Mn_{12} molecules were transferred from the as-loaded sample surface onto the clean Bi(111) film. If Mn_{12} molecules had been deposited onto a Bi(111) film directly from the Mn_{12} solution diluted in IPA, they would have aggregated instead of forming individual Mn_{12} molecules. The efficiency of the tip-deposition method depends on the total scanning time of the W tip on the Mn_{12}-covered HOPG surface. As the scanning time increases, the number of Mn_{12} molecules attached to the W tip increases, and so does the number of Mn_{12} molecules transferred to the Bi substrate. Typically, a bias pulse of 5 V with a scanning time of 30 min can generate tens of individual Mn_{12} molecules covered in a region of several hundred square nanometers.

DFT+U Method. Periodic DFT+U calculations were performed for a Mn_{12} molecule physisorbed on a Bi(111) slab, within the generalized gradient approximation[34] for exchange-correlation functional and projector-augmented wave pseudopotentials,[35] using VASP.[36,37] We used a simplified form of Mn_{12} molecule, $[Mn_{12}O_{12}(COOH)_{16}(H_2O)_4]$, where CH_3 groups in the terminating ligands were replaced by H atoms, in order to save computational time. It was shown that this simplification did not change electronic and magnetic properties of Mn_{12}.[20] We have not included van der Waals interactions. For the flat-lying (side-lying) orientation, we used a supercell consisting of one Mn_{12} molecule on a Bi(111) slab of 4 × 4 × 6 (3 × 3 × 10) atoms, with a vacuum layer of 11 Å. The geometry of Mn_{12} on the Bi slab was optimized with SOC and on-site Coulomb repulsion U = 4 eV for the Mn d electrons only,[20,30] while all the atoms were relaxed except for the bottom-most Bi atomic layer, with an energy cutoff of 400 eV and the Γ point (k = 0), until the magnitude of the maximum force is less than 0.05 eV/Å. Motivated by the STM topographic image, a flat-lying Mn_{12} molecule was initially tilted by 6° relative to the vertical axis. After the geometry relaxation, we found that the tilting angle has not changed. For the almost flat-lying orientation, the shortest vertical z distance between the bottom-most H (O) atom of the Mn_{12} and the Bi atom was initially 1.57 (2.93) Å, while the optimized shortest z value became 1.80 (2.61) Å and the optimized shortest distance is 2.88 (3.54) Å. For the side-lying orientation (Figure S3), the initial shortest z value between the bottom-most H (O) atom of the Mn_{12} and Bi was 1.88 (3.23) Å, while the optimized z value became 1.84 (2.71) Å. This indicates that chemical bonding between the Mn_{12} and the Bi slab is unlikely, which corroborates our experimental findings (Figure S2). Electronic and magnetic properties of a Mn_{12} molecule on Bi(111) were calculated using the optimized geometry for each orientation, including SOC self-consistently, U = 4 eV, and dipole corrections along the z axis. For the flat-lying (side-lying) orientation, we used an energy cutoff of 400 eV and k-points of 3 × 2 × 1 (4 × 3 × 1). The adsorption energy of the flat-lying (side-lying) orientation is 1.42 (0.69) eV. The higher adsorption energy for the flat-lying orientation is consistent with the observation that more Mn_{12} molecules with the flat-lying orientation were found. For both orientations, we found that the HOMO−LUMO gap is greatly reduced and that the total magnetic moment increases by 1 μ_B.

Conflict of Interest: The authors declare no competing financial interest.

Acknowledgment. This work was supported by the National Natural Science Foundation of China (Grant Nos. 10974156, 21173170, 91121013), U.S. National Science Foundation (DMR-0804665, DMR-1206354), and San Diego Supercomputer Center (DMR060009N).

Supporting Information Available: Additional STM images of individual IPA solvent molecules and of the tip-induced disappearance of Mn_{12} molecules showing an intact Bi(111) surface after removal of the Mn_{12} molecules. Schematic geometry and observed STM image and d*I*/d*V* maps for the side-lying orientation, and DFT-calculated total DOS and projected DOS onto all the atoms in the Mn_{12} for the (almost) flat-lying and side-lying orientations. Analysis of the orbitals for the (almost) flat-lying orientation in comparison to the orbitals for an isolated or free Mn_{12} molecule. This material is available free of charge *via* the Internet at http://pubs.acs.org.

REFERENCES AND NOTES

1. Sessoli, R.; Gatteschi, D.; Caneschi, A.; Novak, M. A. Magnetic Bistability in a Metal-Ion Cluster. *Nature* **1993**, *365*, 141–143.
2. Friedman, J. R.; Sarachik, M. P.; Tajeda, J.; Ziolo, J. Macroscopic Measurement of Resonant Magnetization Tunneling in High-Spin Molecules. *Phys. Rev. Lett.* **1996**, *76*, 3830–3833.
3. Wernsdorfer, W.; Sessoli, R. Quantum Phase Interference and Parity Effects in Magnetic Molecular Clusters. *Science* **1999**, *284*, 133–135.
4. Leuenberger, M. N.; Loss, D. Quantum Computing in Molecular Magnets. *Nature* **2001**, *410*, 789–793.
5. Voss, S.; Fonin, M.; Rüdiger, U.; Burgert, M.; Groth, U.; Dedkov, Yu. S. Electronic Structure of Mn_{12} Derivatives on the Clean and Functionalized Au Surface. *Phys. Rev. B* **2007**, *75*, 045102.
6. Voss, S.; Zander, O.; Fonin, M.; Rüdiger, U.; Burgert, M.; Groth, U. Electronic Transport Properties and Orientation of Individual Mn_{12} Single-Molecule Magnets. *Phys. Rev. B* **2008**, *78*, 155403.
7. Kahle, S.; Deng, Z.; Malinowski, N.; Tonnoir, C.; Forment-Aliaga, A.; Thontasen, N.; Rinke, G.; Le, D.; Turkowski, V.; Rahman, T. S.; *et al.* The Quantum Magnetism of Individual Manganese-12-Acetate Molecular Magnets Anchored at Surfaces. *Nano Lett.* **2012**, *12*, 518–521.

8. Cornia, A.; Fabretti, A. C.; Pacchioni, M.; Zobbi, L.; Bonacchi, D.; Caneschi, A.; Gatteschi, D.; Biagi, R.; Del Pennino, U.; Renzi, V. D.; *et al.* Direct Observation of Single-Molecule Magnets Organized on Gold Surfaces. *Angew. Chem., Int. Ed.* **2003**, *42*, 1645–1648.
9. Salman, Z.; Chow, K. H.; Miller, R. I.; Morello, A.; Parolin, T. J.; Hossain, M. D.; Keeler, T. A.; Levy, C. D. P.; MacFarlane, W. A.; Morris, G. D.; *et al.* Local Magnetic Properties of a Monolayer of Mn_{12} Single Molecule Magnets. *Nano Lett.* **2007**, *7*, 1551–1555.
10. Mannini, M.; Pineider, F.; Sainctavit, P.; Moulin, C. C. D.; Arrio, M. A.; Cornia, A.; Gattesch, D.; Sessoli, R. XMCD of a Single Layer of Single Molecule Magnets. *Eur. Phys. J.: Spec. Top.* **2009**, *169*, 167–173.
11. Saywell, A.; Magnano, G.; Satterley, C. J.; Perdigão, L. M. A.; Britton, A. J.; Taleb, N.; del Carmen Giménez-López, M.; Champness, N. R.; O'Shea, J. N.; Beton, P. H. Self-Assembled Aggregates Formed by Single-Molecule Magnets on a Gold Surface. *Nat. Commun.* **2010**, *1*, 75.
12. Del Pennino, U.; Corradini, V.; Biagi, R.; Renzi, V. D.; Moro, F.; Boukhvalov, D. W.; Panaccione, G.; Hochstrasser, M.; Carbone, C.; Milios, C. J.; *et al.* Electronic Structure of a Mn_6 ($S = 4$) Single Molecule Magnet Grafted on Au(111). *Phys. Rev. B* **2008**, *77*, 085419.
13. Mannini, M.; Pineider, F.; Sainctavit, P.; Danieli, C.; Otero, E.; Sciancalepore, C.; Talarico, A. M.; Arrio, M.-A.; Cornia, A.; Gatteschi, D.; *et al.* Magnetic Memory of a Single-Molecule Quantum Magnet Wired to a Gold Surface. *Nat. Mater.* **2009**, *8*, 194–197.
14. Corradini, V.; Moro, F.; Biagi, R.; Renzi, V. D.; Del Pennino, U.; Bellini, V.; Carretta, S.; Santini, P.; Milway, V. A.; Timco, G.; *et al.* Successful Grafting of Isolated Molecular Cr_7Ni Rings on Au(111) Surface. *Phys. Rev. B* **2009**, *79*, 144419.
15. Ghirri, A.; Corradini, V.; Bellini, V.; Biagi, R.; Del Pennino, U.; Renzi, V. D.; Cezar, J. C.; Muryn, C. A.; Timco, G. A.; Winpenny, R. E. P.; *et al.* Self-Assembled Monolayer of Cr_7Ni Molecular Nanomagnets by Sublimation. *ACS Nano* **2011**, *5*, 7090–7099.
16. Heersche, H. B.; de Groot, Z.; Folk, J. A.; van der Zant, H. S. J.; Romeike, C.; Wegewijs, M. R.; Zobbi, L.; Barreca, D.; Tondello, E.; Cornia, A. Electron Transport through Single Mn_{12} Molecular Magnets. *Phys. Rev. Lett.* **2006**, *96*, 206801.
17. Zyazin, A. S.; van den Berg, J. W. G.; Osorio, E. A.; van der Zant, H. S. J.; Konstantinidis, N. P.; Leijnse, M.; Wegewijs, M. R.; May, F.; Hofstetter, W.; Danieli, C.; *et al.* Electric Field Controlled Magnetic Anisotropy in a Single Molecule. *Nano Lett.* **2010**, *10*, 3307–3311.
18. Jo, M.-H.; Grose, J. E.; Baheti, K.; Deshmukh, M. M.; Sokol, J. J.; Rumberger, E. M.; Hendrickson, D. N.; Long, J. R.; Park, H.; Ralph, D. C. Signatures of Molecular Magnetism in Single-Molecule Transport Spectroscopy. *Nano Lett.* **2006**, *6*, 2014–2020.
19. Barraza-Lopez, S.; Park, K.; García-Suárez, V.; Ferrer, J. First-Principles Study of Electron Transport through the Single-Molecule Magnet Mn_{12}. *Phys. Rev. Lett.* **2009**, *102*, 246801.
20. Barraza-Lopez, S.; Avery, M. C.; Park, K. First-Principles Study of a Single-Molecule Magnet Mn_{12} Monolayer on the Au(111) Surface. *Phys. Rev. B* **2007**, *76*, 224413.
21. Vitali, L.; Fabris, S.; Conte, A. M.; Brink, S.; Ruben, M.; Baroni, S.; Kern, K. Electronic Structure of Surface-Supported Bis-(phthalocyaninato) Terbium(III) Single Molecular Magnets. *Nano Lett.* **2008**, *8*, 3364–3368.
22. Martínez, R. V.; García, F.; García, R.; Coronado, E.; Forment-Aliaga, A.; Romero, F. M.; Tatay, S. Nanoscale Deposition of Single-Molecule Magnets onto SiO_2 Patterns. *Adv. Mater.* **2007**, *19*, 291–295.
23. Thayer, G. E.; Sadowski, J. T.; Heringdorf, F. M. Z.; Sakurai, T.; Tromp, R. M. Role of Surface Electronic Structure in Thin Film Molecular Ordering. *Phys. Rev. Lett.* **2005**, *95*, 256106.
24. Hirahara, T.; Nagao, T.; Matsuda, I.; Bihlmayer, G.; Chulkov, E. V.; Koroteev, Y. M.; Echenique, P. M.; Saito, M.; Hasegawa, S. Role of Spin-Orbital Coupling and Hybridization Effects in the Electronic Structure of Ultrathin Bi Film. *Phys. Rev. Lett.* **2006**, *97*, 146803.
25. Kevan, S. D.; Gaylord, R. H. High-Resolution Photoemission Study of the Electronic Structure of the Noble-Metal (111) Surface. *Phys. Rev. B* **1987**, *36*, 5809–5818.
26. Anisimov, V. I.; Aryasetiawan, F.; Lichtenstein, A. I. First-Principles Calculations of the Electronic Structure and Spectra of Strongly Correlated Systems: The LDA+U Method. *J. Phys.: Condens. Matter* **1997**, *9*, 767–808.
27. Tersoff, J.; Hamann, D. R. Theory and Application for the Scanning Tunneling Microscope. *Phys. Rev. Lett.* **1983**, *50*, 1998–2001.
28. Tersoff, J.; Hamann, D. R. Theory and Application for the Scanning Tunneling Microscope. *Phys. Rev. B* **1985**, *31*, 805–813.
29. Park, K.; Wang J.-Z. Significant Charge Transfer between a Single-Molecule Magnet Mn_{12} and a Bi Substrate. *Polyhedron* **2013**, http://dx.doi.org/10.1016/j.poly.2013.03.021.
30. Boukhvalov, D. W.; Al-Saqer, M.; Kurmaev, E. Z.; Moewes, A.; Galakhov, V. R.; Finkelstein, L. D.; Chiuzbăian, S.; Neumann, M.; Dobrovitski, V. V.; Katsnelson, M. I.; *et al.* Electronic Structure of a Mn_{12} Molecule Magnet: Theory and Experiment. *Phys. Rev. B* **2007**, *75*, 014419.
31. Koroteev, Y. M.; Bihlmayer, G.; Gayone, J. E.; Chulkov, E. V.; Blugel, S.; Echenique, P. M.; Hofmann, P. Strong Spin−Orbit Splitting on Bi Surfaces. *Phys. Rev. Lett.* **2004**, *93*, 046403.
32. Hofmann, P. The Surfaces of Bismuth: Structural and Electronic Properties. *Prog. Surf. Sci.* **2006**, *81*, 191–245.
33. Lis, T. Preparation, Structure, and Magnetic Properties of a Dodecanuclear Mixed-Valence Manganese Carboxylate. *Acta Crystallogr., Sect. B: Struct. Crystallogr. Cryst. Chem.* **1980**, *36*, 2042–2046.
34. Perdew, J. P.; Burke, K.; Ernzerhof, M. Generalized Gradient Approximation Made Simple. *Phys. Rev. Lett.* **1996**, *77*, 3865–3868.
35. Blochl, P. E. Project Augmented-Wave Method. *Phys. Rev. B* **1994**, *50*, 17953–17959.
36. Kresse, G.; Furthmuller, J. Efficient Iterative Schemes for *Ab-Initio* Total-Energy Calculations Using a Plane-Wave Basis Set. *Phys. Rev. B* **1996**, *54*, 11169–11186.
37. Kresse, G.; Furthmuller, J. Efficiency of *Ab-Initio* Total Energy Calculations for Metals and Semiconductors Using a Plane-Wave Basis Set. *Comput. Mater. Sci.* **1996**, *6*, 15–50.